# AVIATION TRANSPORT

UDC 004.932.72’1(045)
DOI:10.18372/1990-5548.86.20627

[1]A. V. Riabko,
[2]V. Y. Hrishnenko

## COMPARATIVE ANALYSIS OF SATELLITE IMAGES STITCHING METHODS BASED ON LOCAL FEATURE DETECTION

Faculty of Air Navigation, Electronics and Telecommunications,
State University “Kyiv Aviation Institute”, Kyiv, Ukraine
E-mails: [1]2383870@stud.kai.edu.ua ORCID 0009-0005-5552-7197,
[2]1744220@stud.kai.edu.ua ORCID 0009-0001-8496-897X

***Abstract*—*This paper investigates feature-based methods for satellite image stitching under a unified evaluation framework. Four algorithms – SIFT, SURF, ORB and BRISK - are examined with respect to keypoint detection, descriptor formation, correspondence generation and geometric alignment. A standardized MATLAB workflow is employed: grayscale detection and description, nearest-neighbour matching with a ratio test, robust outlier rejection via RANSAC with model escalation and mask-based blending with content cropping. Approximately fifty image sets spanning diverse landforms are processed; a Sahara Desert example illustrates the protocol. The study’s aim is to characterize the accuracy-efficiency trade-offs of vector (SIFT, SURF) and binary (ORB, BRISK) descriptors in realistic orbital conditions and to provide a transparent basis for method selection in remote-sensing workflows.*

**Keywords**—Satellite image stitching; remote sensing; image registration; local feature detection; SIFT; SURF; ORB; BRISK; vector descriptors; binary descriptors; feature matching.

### I. INTRODUCTION

Satellite images are behind all the current mapping, environmental monitoring, disaster response and defense planning. These data generate mostly from the unaligned frames due to acquisition at different times, view angles and illumination [1]. The reliable image stitching, thus, is the one that can convert such streams into seamless mosaics so that rivers kind of form lines, roads sort of merge and boundaries are definitely sharp. The quality of that stitching controls what further analyses can use and measure.

Stitching in the remote-sensing setting is harder than in ground photography. Terrain relief, off-nadir viewing, radiometric drift, seasonal change and atmospheric haze all distort appearance. Overlap can be small or irregular and man-made patterns such as rooftops or field grids introduce repeated textures that confuse naive matchers [2]. Any practical method must therefore find features that survive scale changes, rotations and modest brightness shifts, then reject outliers before estimating the geometric warp.

This study examines stitching principles built on local feature detectors and descriptors. Two families are compared. Scale-Invariant Feature Transform (SIFT) and Speeded-Up Robust Features (SURF) produce descriptors with rich gradient statistics. Oriented FAST and Rotated BRIEF (ORB) and Binary Robust Invariant Scalable Keypoints (BRISK) yield compact binary descriptors optimized for speed and memory. All four algorithms widely used design points: high-dimension vectors versus lightweight binary codes [3].

To make the comparison fair, the surrounding is kept constant. Keypoints are detected across scale, descriptors are extracted, putative matches are formed with a ratio test and outliers are removed by Random Sample Consensus (RANSAC). Warps are estimated in an escalating model class – similarity, affine and, if required, projective – to accommodate viewpoint and relief [4].

Evaluation focuses on alignment accuracy and efficiency that matter in practice. Reported measures include match count, inlier count and inlier ratio after RANSAC, match density per unit overlap and repeatability under controlled rotations and brightness shifts. All experiments are run in MATLAB using the same pre-processing and blending stages, so that differences can be attributed to the detector – descriptor choice.

The goal is a clear, evidence-based view of when vector descriptors justify their cost and when binary descriptors are sufficient at scale. By grounding the analysis in satellite scenes with realistic variation, the paper aims to inform method selection for mapping, change detection and large-area mosaicking where both accuracy and throughput are basic principles of satellite images stitching.

## II. Strengths and Limitations of Feature-Based Registration for Satellite Mosaicking

Satellite image stitching sits at a crossroads between two active lines of research: classical, feature-based registration and newer, learned (deep) matchers. In operational mosaicking stitching is still framed as a sequence of registration, seamline selection, tone normalization and blending – each step sensitive to side-looking geometry, relief, seasonal change and radiometric drift that are common in orbital data. Recent remote-sensing papers continue to refine every stage, from robust registration to seam generation for large orthoimage mosaics and time-series products [5].

Feature-based stitching remains attractive because it is transparent, lightweight and easy to adapt across sensors. Local keypoints are detected over scale, described, matched with a ratio test and filtered with RANSAC before estimating similarity / affine / projective warps; the approach scales well and gives explicit geometric guarantees. Its main liabilities are brittle matching under low texture, repetitive patterns, large viewpoint or illumination changes and cross-modal pairs [6]. Survey articles in remote sensing echo these trade-offs and report steady, incremental progress on detectors, descriptors and robust estimators [7].

The deep-learning track pushes in the opposite direction: learn detectors, descriptors and even correspondence maps end-to-end. Methods based on SuperPoint / LightGlue, SuperGlue, LoFTR and newer transformer variants lift performance under appearance change and wide baselines and are spreading to aerial/satellite regimes; however, they demand more compute, large training sets and often benefit from domain-specific fine-tuning [8]. Recent reviews document the shift from detector-based to detector-free matchers and their gains, while satellite-focused studies show practical approaches that combine learned features with careful batching and radiometric pre-processing [9].

In this study, the emphasis is on four workhorses: SIFT (Scale-Invariant Feature Transform), SURF (Speeded-Up Robust Features), ORB (Oriented FAST and Rotated BRIEF) and BRISK (Binary Robust Invariant Scalable Keypoints). These methods remain attractive in remote sensing because they expose every decision – keypoint detection, descriptor formation, matching and outlier removal – and they run reliably across sensors and scenes without large training sets.

SIFT and SURF represent the vector descriptor family. They encode gradients in floating-point histograms that are robust to scale and rotation and reasonably tolerant to illumination drift. In stitching, that extra distinctiveness pays off when overlaps are small, terrain relief introduces parallax or seasonal change alters appearance. The trade-off is cost: larger descriptors, heavier memory traffic and longer matching times. With ratio tests and RANSAC, SIFT / SURF matches often yield higher inlier counts and more stable transforms, which reduces seam artifacts and deformation in the final mosaic.

ORB and BRISK sit in the binary descriptor camp. They create compact bit strings using intensity comparisons, then match with Hamming distance. The benefits are clear for large scenes and long strips: far lower memory use, fast nearest-neighbour search and easy batching. ORB couples FAST keypoints with oriented, rotated BRIEF (rBRIEF), while BRISK adds a scale-space detector and a learned sampling pattern to improve rotation and scale tolerance. In wide-area stitching, these designs deliver high throughput and competitive coverage; the cost is reduced distinctiveness under severe viewpoint changes, repetitive textures (e.g., roofs or crop grids) or strong radiometric shifts. Careful thresholding, cross-checks and geometric verification help close that gap [10], [11].

Across these four methods, the intent of using local features is consistent: obtain reliable, spatially well-distributed tie points that survive downsampling, rotation and moderate illumination change; filter mismatches with a ratio test and RANSAC; then estimate the simplest warp that explains the inliers (similarity → affine → projective). For evaluation, the community converges on practical indicators: total matches, inlier count and inlier ratio after RANSAC, match density per overlap area and repeatability under controlled rotations/brightness changes [12].

## III. The Operational Algorithms of SIFT/SURF and BRISK/ORB Methods

Accurate geometric registration across scenes taken at various times, viewing angles and radiometric circumstances is essential for satellite picture stitching. The very first actions in a feasible image stitching process are identification of prominent and well-localized points that can survive through scale and rotation, encoding of their surrounding areas into robust yet peculiar descriptors and reliable correspondence of points in different images for the purpose of estimating a global warp [13]. This chapter describes the algorithmic workings of four popular approaches: ORB, BRISK, SURF and SIFT. BRISK and ORB generate compact binary descriptors based on intensity comparisons, while SIFT and SURF generate floating-point (vector) descriptors based on image gradients and Haar replies.

SIFT established the modern template for invariant local features. Its design targets three properties critical for satellite mosaicking: stability under scale change, consistent orientation in the presence of rotations and descriptive power in textured yet repetitive scenes. Because satellite datasets often mix resolutions and view angles, SIFT's explicit scale space, orientation normalization and high-dimensional gradient statistics make it a strong baseline for reliable points.

SIFT constructs a Gaussian scale space by convolving the image $I(x, y)$ with filters of increasing standard deviation $\sigma$:

$$L(x, y, \sigma) = G(x, y, \sigma) I(x, y), \tag{1}$$

$$G(x, y, \sigma) = \frac{1}{2\pi\sigma^2} e^{\frac{-(x^2+y^2)}{2\sigma^2}}, \tag{2}$$

Keypoints are located as extrema of the Difference-of-Gaussians (DoG):

$$DoG(x, y, \sigma) = L(x, y, k\sigma) - L(x, y, \sigma), \tag{3}$$

where each sample compared to its 26 neighbours in a 3×3×3 neighbourhood across $(x, y, \sigma)$.

Candidate locations are refined by a second-order Taylor expansion of $D$ around the discrete extremum. Low-contrast points and edge-like responses (identified via the Hessian's eigenvalue ratio) are rejected to improve repeatability on satellite textures.

Rotation invariance is achieved by building a 36-bin histogram of gradient directions within a circular, scale-proportional window around the keypoint. For each pixel, compute:

$$m = \sqrt{L_x^2 - L_y^2}, \quad \theta = \operatorname{atan2}(L_y, L_x), \tag{4}$$

and add $m$ to the bin at $\theta$, with additional Gaussian spatial weighting. Secondary peaks that reach at least 0.8 of the main peak yield duplicate keypoints with multiple orientations, improving robustness in complex neighborhoods.

Gradients are sampled in a patch aligned to the dominant orientation and partitioned into a 4×4 grid; each cell contributes an 8-bin histogram, forming a 128-D vector. The descriptor is normalized, clamped and renormalized to reduce contrast sensitivity.

Descriptors are compared by Euclidean distance. The ratio test (nearest vs. second-nearest) rejects ambiguous matches before robust geometric estimation on remaining pairs.

SURF follows SIFT's structure but was engineered to cut computation for large images – exactly the need in orbital mapping. By replacing continuous Gaussian derivatives with box-filter approximations evaluated through integral images, SURF preserves much of SIFT's invariance while improving throughput on wide scenes and long strips.

SURF detects interest points using the Hessian matrix of the scale space:

$$H(x, \sigma) = \begin{bmatrix} L_{xx}(x, \sigma) & L_{xy}(x, \sigma) \\ L_{yx}(x, \sigma) & L_{yy}(x, \sigma) \end{bmatrix}, \tag{5}$$

Second-order derivatives are approximated with rectangular box filters evaluated via integral images. Let $L_{xx}, L_{yy}, L_{xy}$ be the corresponding box-filter responses; SURF scores saliency by a weighted determinant:

$$\det(H) = L_{xx} L_{yy} - (L_{xy})^2. \tag{6}$$

Then seeks 3D extrema in a 3×3×3 neighbourhood across $(x, y, \sigma)$.

Rather than downsampling the image, SURF increases filter sizes to traverse scale, which preserves localization at native resolution – useful when ground sampling distance varies across scenes. Orientation is derived from Haar-wavelet responses $(d_x, d_y)$ in a circular window proportional to σ. A sliding angular sector accumulates the vector sum $\left(\sum d_x, \sum d_y\right)$; the sector with the largest norm defines the dominant angle.

In a patch aligned to the dominant orientation, SURF aggregates Haar responses over a 4×4 grid. Each cell contributes a short vector (e.g., $\left(\sum d_x, \sum d_y, \sum |d_x|, \sum |d_y|\right)$ yielding a 64-D or 128-D descriptor depending on variant. Matching proceeds with Euclidean distance and the ratio test, followed by robust model fitting [15].

ORB was designed for real-time vision on constrained hardware. In satellite stitching, where scenes can span hundreds of megapixels, the ability to detect and match features quickly with modest memory is a practical advantage. ORB achieves this by combining a fast corner detector with an efficient, rotation-aware binary descriptor.

ORB begins with FAST detection over a multi-level pyramid (parameters such as scale factor and number of levels govern the scale range). Because FAST does not score “cornerness,” ORB ranks candidates with a Harris-type response derived from the second-moment matrix:

$$M = \begin{bmatrix} \sum I_x^2 & \sum I_x I_y \\ \sum I_x I_y & \sum I_y^2 \end{bmatrix}, \tag{7}$$

$$R = \det(m) - k \cdot \left(trace(M)\right)^2, \tag{8}$$

with $k \in [0.04, 0.06]$. Points with high $R$ are retained to improve stability on patterns common in satellite scenes. ORB computes geometric moments within a scale-proportional window and employs a rotation-aware BRIEF. Each bit compares two Gaussian-smoothed samples at rotated offsets:

$$\tau(p;x,y) = \begin{cases} 1, \text{ if } I(p+x) < I(p+y), \\ 0, \text{ else.} \end{cases} \tag{9}$$

where $p$ is the keypoint coordinates; $x$ and $y$ is the offset within the selected window. The pair set is learned to maximize bit variance and minimize inter-bit correlation, yielding a 256-bit descriptor with strong speed - accuracy balance.

Descriptors are compared by Hamming distance. In practice, $k$-nearest neighbours with a Hamming-ratio test provides robust candidate pairs prior to geometric verification.

BRISK extends the binary-descriptor idea to better handle scale changes and rotations found in aerial and orbital imagery. It pairs a multiscale corner detector with a carefully arranged sampling pattern, separating long-range comparisons for orientation from short-range comparisons for the descriptor itself.

BRISK detects candidates with FAST across a scale pyramid and refines them to subpixel and subscale precision by quadratic interpolation of the detector response in:

$$\hat{x} = -H^{-1} \cdot g, \tag{10}$$

where $H$ and $g$ are the first- and second-order derivatives of the response. This improves repeatability under downsampling and oblique viewing.

Around each keypoint, BRISK places sampling points on concentric circles. “Long-range” pairs estimate orientation via a smoothed intensity differential which defines the canonical rotation for the descriptor.

“Short-range” pairs produce the descriptor bits by simple intensity tests at the rotation-aligned locations. A common configuration yields 512 bits, matched efficiently with Hamming distance.

As with ORB, nearest-neighbour search under Hamming distance supplies putative correspondences. A ratio test and cross-check reduce ambiguities before robust model estimation [16].

## IV. Methods Comparison and Evaluation

This section assesses four methods based on local features such as SIFT, SURF, ORB and BRISK for the stitching of satellite images through a single workflow that combines registration and blending. The comparison is decided on the basis of the implementation: every method operates in the same MATLAB The Image Processing Toolbox environment with exactly the same pre- and post-processing steps. Each pair or group of overlapping images is first turned to grayscale for the detection and description, whereas the original RGB data is used for visualization. Putative matches are created by means of a ratio test, then filtered through robust estimation and finally are used to determine a geometric warp. To avoid bias toward any single model, the transform escalates from similarity to affine and, when necessary, to projective, with RANSAC controlling inlier selection and outlier rejection. The stitched mosaic is created through mask-based compositing and then cut to its content support, which enables the quantitative measurements to represent only the areas that have data overlap.

Across approximately fifty experimental runs on diverse satellite scenes – urban cores, suburban blocks, agricultural parcels, coastal strips and mountainous terrain – the identical stitching workflow was applied and the same metrics were recorded. Parameter settings, model escalation and blending were held constant to isolate the effect of the detector–descriptor choice. For the sake of keeping the presentation on point, one case that represents the whole is shown below; it illustrates the entire procedure and the method of calculating the metrics. Aggregate results across the full set are consistent with the trends observed in this example.

The dataset with four Sahara satellite images (Figs 1 – 4) was used for example as it combines large homogeneous areas with highly structured landforms. Broad sand sheets and playa surfaces impose low local contrast, which stresses detector repeatability. At the same time, dune fields, basalt outcrops, escarpments supply sharp, high-frequency edges and corners that reward truly distinctive descriptors.

Because all four methods (SIFT, SURF, ORB, BRISK) produced visually consistent mosaics on the Sahara set – comparable seam placement, minimal residual parallax and similar inlier ratios within a narrow margin – for brevity, the Fig. 5 presents a single representative stitch.

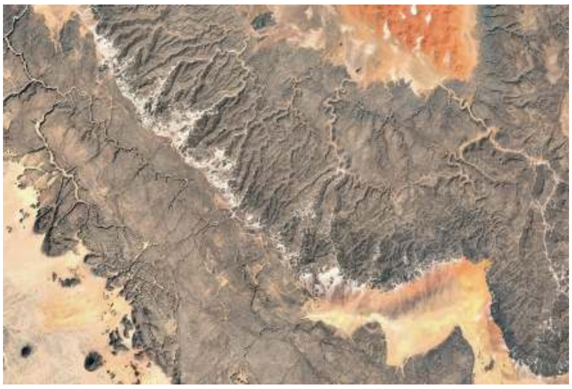

Fig. 1. Sahara Desert satellite image #1

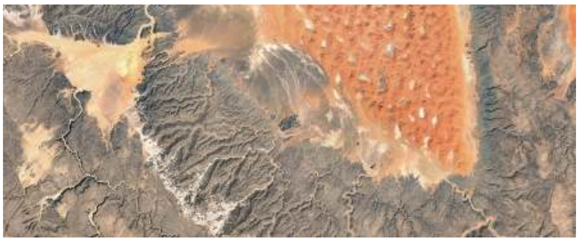

Fig. 2. Sahara Desert satellite image #2

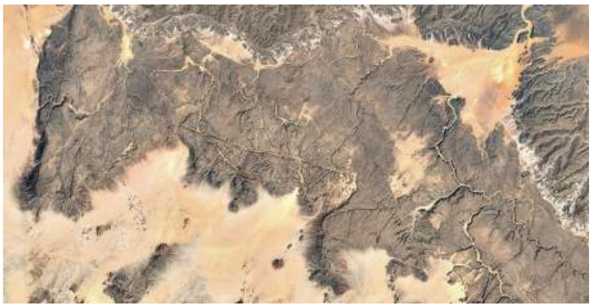

Fig. 3. Sahara Desert satellite image #3

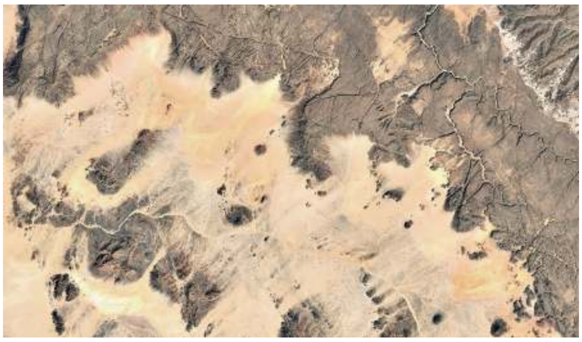

Fig. 4. Sahara Desert satellite image #4

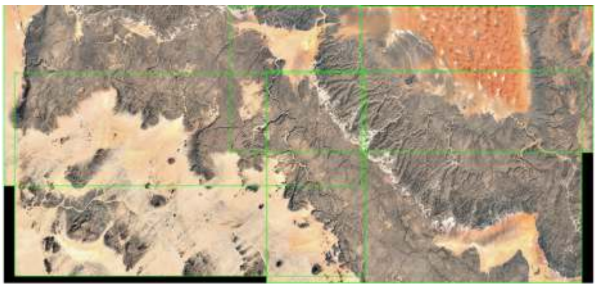

Fig. 5. Result of Sahara Desert satellite images stitching

Figure 6 shows raw match density. This graph defines the total number of feature matches divided by the total number of overlap pixels across the stitched area. This normalization removes scale and crop effects, so methods can be compared on a per-pixel basis even when images differ in size or overlap.

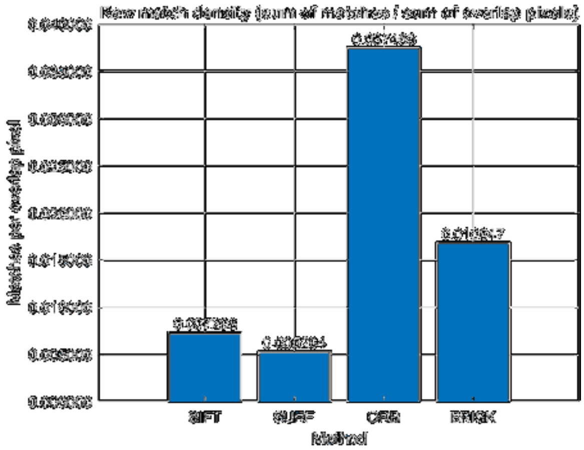


Fig. 6. Match density per method

Numerically, ORB attains the highest density (≈ 0.0375), followed by BRISK (≈ 0.0168), with SIFT (≈ 0.0073) and SURF (≈ 0.0053) lower by a substantial margin. This pattern is consistent with descriptor design: binary descriptors (ORB, BRISK) generate more candidates per unit area because Hamming matching is inexpensive and the codes are compact, whereas vector descriptors (SIFT, SURF) are more selective and computationally heavier.

## V. Conclusions

In a controlled stitching workflow applied to roughly fifty satellite image pairs, all four methods - SIFT, SURF, ORB and BRISK – produced reliable mosaics when overlap and scene structure were adequate. The methods differed, however, in how they reached that result. ORB and BRISK delivered the highest raw match density per overlap pixel and the fastest runtimes, reflecting the efficiency of binary descriptors and Hamming search. SIFT and SURF yielded lower match densities but consistently stronger inlier ratios. On the Sahara example, where all four aligned well, a single stitched image sufficed to illustrate the workflow; method-level counts still showed the same accuracy.

For large-area mapping where speed and memory dominate, start with ORB or BRISK to harvest many candidates ties quickly. For challenging geometry or radiometry – small overlaps, repetitive urban grids, low-contrast expanses, seasonal drift - prefer SIFT or SURF, which buy distinctiveness and higher inlier reliability at greater computational cost.

## REFERENCES

[1] M. Ivanytskyi, Y. Averyanova, N. Sauliak, and Y. Znakovska, "Machine learning-driven UAV mapping for automated detection of nutritional deficiencies and diseases in wheat," *CEUR Workshop Proceedings*, Conference Paper, State University Kyiv Aviation Institute, 2025.

[2] M. Brown and D. G. Lowe, "Automatic panoramic image stitching using invariant features," *International Journal of Computer Vision*, vol. 74, no. 1, pp. 59–73, 2007. https://doi.org/10.1007/s11263-006-0002-3

[3] D. G. Lowe, "Distinctive image features from scale-invariant keypoints," *International Journal of Computer Vision*, 60 (2), pp. 91–110, 2004. https://doi.org/10.1023/B:VISI.0000029664.99615.94

[4] B. Zitová, J. Flusser, "Image registration methods: A survey," *Image and Vision Computing*, vol. 21, no. 11, pp. 977–1000, 2003. https://doi.org/10.1016/S0262-8856(03)00137-9

[5] G. Malini and R. Radha, "Comparative analysis of various feature extracting algorithms using satellite images," *Journal of Advanced Research in Dynamical and Control Systems*, vol. 12, Issue 7, pp. 545–552, 2020. https://doi.org/10.5373/JARDCS/V12SP7/20202138

[6] J. Chon, H. Kim, and C.-S. Lin, "Seam-line determination for image mosaicking: A technique minimizing the maximum local mismatch and the global cost," *ISPRS Journal of Photogrammetry and Remote Sensing*, vol. 65, pp. 86–92, 2010. https://doi.org/10.1016/j.isprsjprs.2009.09.001

[7] G. Chen, M. Sun, X. Hu, and Z. Zhang, "Optimal seamline detection for orthoimage mosaicking based on DSM and improved JPS algorithm," *Remote Sensing*, vol. 10, no. 6, 821, 2018. https://doi.org/10.3390/rs10060821

[8] L. Li, L. Han, Y. Ye, Y. Xiang, and T. Zhang, "Deep learning in remote sensing image matching: A survey," ISPRS Journal of Photogrammetry and *Remote Sensing*, vol. 225, pp. 88–112, 2025. https://doi.org/10.1016/j.isprsjprs.2025.04.001

[9] X. Li, N. Hui, H. Shen, Y. Fu, and L. Zhang, "A robust mosaicking procedure for high spatial resolution remote sensing images," *ISPRS Journal of Photogrammetry and Remote Sensing*, vol. 109, pp. 108–125, 2015. https://doi.org/10.1016/j.isprsjprs.2015.09.009

[10] X. Yu, J. Pan, S. Chen, and M. Wang, "A flexible multi-temporal orthoimage mosaicking method based on dynamic variable patches," *Information Fusion*, vol. 108, Article number 102350, 2024. https://doi.org/10.1016/j.inffus.2024.102350

[11] P. S. Tondewad and M. P. Dale, "Remote Sensing Image Registration Methodology: Review and Discussion," *Procedia Computer Science*, vol. 171, pp. 2390–2399, 2020. https://doi.org/10.1016/j.procs.2020.04.259

[12] X. Zhang, C. Leng, Y. Hong, Z. Pei, I. Cheng, and A. Basu, "Multimodal Remote Sensing Image Registration Methods and Advancements: A Survey," *Remote Sensing*, vol. 13, no. 24, Article number 5128, 2021. https://doi.org/10.3390/rs13245128 \

[13] J. Pan, Q. Zhou, and M. Wang, "Seamline determination based on segmentation for urban image mosaicking," *IEEE Geoscience and Remote Sensing Letters*, vol. 11, no. 8, pp. 1335–1339, 2014. https://doi.org/10.1109/LGRS.2013.2293197

[14] A. Riabko, "Methods of satellite images segmentation analysis," 7th IEEE International *Conference on Methods and Systems of Navigation and Motion Control (MSNMC),* Kyiv, Ukraine, 2023, pp. 163–167. https://doi.org/10.1109/MSNMC61017.2023.10329167

[15] A. Riabko, "Comparative analysis of SIFT and SURF methods for local feature detection in satellite imagery", *2024 International Workshop on Computational Methods in Systems Engineering, (CMSE 2024),* National Aviation University, Kyiv, Ukraine, vol. 3732, pp. 21–31. ISSN: 16130073.

[16] A. Riabko and V. Hrishnenko "Comparative analysis of BRISK and ORB methods for local feature detection in satellite imagery", *Electronics and Control Systems*, National Aviation University, Kyiv, Ukraine, no 1(83), pp. 44–53, 2025. ISSN 1990-5548. https://doi.org/10.18372/1990-5548.83.19879

Received September 25, 2025

**Riabko Artem.** ORCID 0009-0005-5552-7197. Postgraduate student.
Faculty of Air Navigation, Electronics and Telecommunications, State University "Kyiv Aviation Institute", Kyiv, Ukraine.
Education: National Aviation University, Kyiv, Ukraine, (2017).
Research area: computer vision.
Publications: 9.
E-mail: 2383870@stud.kai.edu.ua

**Hrishnenko Vitalii.** ORCID 0009-0001-8496-897X. Postgraduate student.
Faculty of Air Navigation, Electronics and Telecommunications, State University "Kyiv Aviation Institute", Kyiv, Ukraine.
Education: National Technical University of Ukraine "Igor Sikorsky Kyiv Polytechnic Institute", Kyiv, Ukraine, (2017).
Research area: data processing.
Publications: 5.
E-mail: 1744220@stud.kai.edu.ua

**А. В. Рябко, В. Ю. Грішненко. Порівняльний аналіз методів зшивання супутникових зображень на основі виявлення локальних ознак**

У роботі досліджено методи зшивання супутникових зображень на основі локальних ознак у межах єдиної оціночної структури. Розглянуто чотири алгоритми – SIFT, SURF, ORB та BRISK – з погляду виявлення ключових точок, формування дескрипторів, генерування відповідностей та геометричного вирівнювання. Використано стандартизований робочий процес у MATLAB: виявлення та опис у відтінках сірого, пошук найближчих сусідів із перевіркою співвідношення, надійне відхилення викидів за допомогою RANSAC із ескалацією моделі та злиття зображень із використанням масок і обрізанням контенту. Було оброблено близько п'ятдесяти наборів зображень, що охоплюють різноманітні типи ландшафтів; приклад із пустелі Сахара ілюструє запропонований протокол. Метою дослідження є охарактеризувати компроміс між точністю та ефективністю для векторних (SIFT, SURF) і бінарних (ORB, BRISK) дескрипторів у реалістичних орбітальних умовах та забезпечити прозору основу для вибору методів у процесах дистанційного зондування.

**Ключові слова**: зшивання супутникових зображень; дистанційне зондування; реєстрація зображень; виявлення локальних ознак; SIFT; SURF; ORB; BRISK; векторні дескриптори; бінарні дескриптори; співставлення ознак.

**Рябко Артем Вікторович.** ORCID 0009-0005-5552-7197. Аспірант.
Факультет аеронавігації, електроніки та телекомунікацій, Державний університет «Київський авіаційний інститут», Київ, Україна.
Освіта: Національний авіаційний університет, Київ, Україна, (2017).
Напрям наукової діяльності: комп'ютерний зір.
Кількість публікацій: 9.
E-mail: 2383870@stud.kai.edu.ua

**Грішненко Віталій Юрійович.** ORCID 0009-0001-8496-897X. Аспірант.
Факультет аеронавігації, електроніки та телекомунікацій, Державний університет «Київський авіаційний інститут», Київ, Україна.
Освіта: Національний технічний університет України «КПІ імені Ігоря Сікорського», Київ, Україна, (2017).
Напрям наукової діяльності: обробка даних.
Кількість публікацій: 5.
E-mail: 1744220@stud.kai.edu.ua